Shuang LI, Zhixin WANG, Guoqiang WANG

School of Electronic Information and Electrical Engineering, Shanghai Jiaotong University

Input-Output Linearization and Predictive Current Controller for Offshore Wind Farm VSC-HVDC

Abstract. *In this paper, a nonlinear controller for VSC-HVDC transmission system is proposed. The feedback linearization based nonlinear differential-geometric techniques is used to cancel nonlinearities and decouple the input control variables. A predictive current control (PCC) method is also proposed. It can predict the current reference for the next sampling instant rapidly and accurately. Comprehensive time-domain computer simulations within MATLAB/Simulink have been carried out and the results show the feasibility and effectiveness of the proposed control scheme.*

Streszczenie. *W artykule przedstawiono algorytm sterowania nieliniowego dla system przesyłu energii VSC-HVDC. W celu odprzężenia sterowanych zmiennych i eliminacji nieliniowości, zastosowano technikę nieliniowej geometrii-różniczkowej do linearyzacji sprzężenia zwrotnego. Zaproponowano także sterowanie predykcyjne prądu. Wykonane badania symulacyjne w programie Matlab/Simulink potwierdziły skuteczność algorytmu sterowania. (**System sterowania dla farm wiatrowych w układzie VSC-HVDC – linearyzacja wejścia/wyjścia, sterowanie predykcyjne prądu**).*

Keywords: feedback linearization; predictive current control (PCC); VSC-HVDC; linear estimate.
Słowa kluczowe: linearyzacja sprzężenie, sterowanie predykcyjne prądu (PCC), VSC-HVDC, estymacja liniowa.

Introduction

With the growing energy demand and environmental pollution problem, the renewable alternative energy such as solar power, wind energy has been attracted more attention all over the world in recent years. Three-phase pulse-width modulation (PWM) voltage-source converters (VSC) using the state-of-the-art power electronic devices, such as insulated-gate bipolar transistor (IGBT), have been applied to offshore wind power generation system for the grid interconnection [1, 2].

As compared to traditional HVDC transmission system, the VSC-HVDC has the attractive features such as almost sinusoidal input currents, controllable input power factor, constant DC-link voltage and bidirectional power flow ability with separately control of active and reactive power [3, 4]. All these features make the VSC-HVDC systems suitable for connecting the offshore wind power to the mains grid [5].

Many research have been done from the control point of view [6, 7], most of those results relay on either using small-signal stability or linearized models with compensation. Their performances will retain under certain conditions such as limited operation range and large DC-link capacitance. Certainly, it is difficult to achieve ideal control effects with linear control theories for the multivariable control inputs and highly coupled nonlinearity of the VSC-HVDC. By dint of its structure, nonlinear control theories based on the input-output linearization (IOL) have been developed over recent years and achieved considerable successes [8, 9]. The feedback linearization is particularly useful in power electronics to tackle the nonlinear problem [10, 11]. The technique is widely used while developing the control for electric machines, such as the permanent-magnet synchronous machine using power electronics converters where a nonlinear process is transformed into a linear one by forcing the output to follow the input in a closed-loop fashion. The major merit of this technique is that one can find a global feedback law to linearize and decouple multi-input multi-output (MIMO) nonlinear system where regular linear design methods can be applied [12, 13].

Usually, dual closed-loop control structure is widely used to control the VSC. Namely, the inner current loop and outer voltage loop. The out loop voltage can be controlled with IOL. The inner current loop has a fast current response, preventing current overflow, follow the input reference current [14]. For a digital-signal-processor (DSP) based controller, there exists the sampling and control delays which will affect the dynamic performance of the VSC. In order to eliminate the static error and discretization error, a new predictive current controller is presented in this paper.

The nonlinear mathematical model of the VSC-HVDC transmission converters is presented in this paper. The IOL technique developed from differential-geometric theory [11, 12], have been applied to the outer voltage control loop. Followed by is the predictive current control (PCC) inner current loop. Several computer simulation results illustrate the effectiveness of the proposed controller. Finally, a conclusion is drawn.

Mathematical model of the VSC-HVDC transmission system

Two VSC stations constitute a typical VSC-HVDC system. Usually, one station at the offshore side operates as the rectifier station whereas the onshore side one operates as the inverter station as shown in Fig.1. The VSCs at both ends control the active power and dc voltage, respectively. Meanwhile, the reactive power is controlled by both ends. They are coordinated operation. The operating mode that active power is controlled by wind farm side VSC1 and DC-link voltage is controlled by grid side VSC2 is adopted in this paper and the reactive power is controlled at both ends at the same time. The main circuit structure of VSC at both ends is the same (as shown in Fig.2) and their control system structure is symmetrical. Therefore, take the system at one end as an example and the other one is the same.

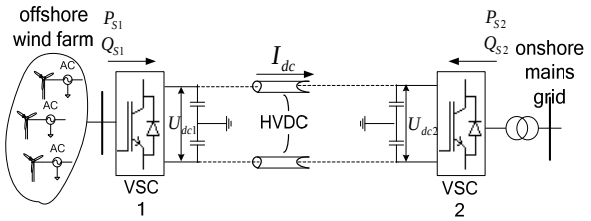

Fig.1 single-line diagram of offshore wind farm VSC-HVDC

The mathematical model developed in this paper can be expressed in the two-phase stationary coordinate system as [15]

(1)
$$\begin{cases} L\dfrac{\mathrm{d}i_\alpha}{\mathrm{d}t} = e_\alpha - v_\alpha - Ri_\alpha \\ L\dfrac{\mathrm{d}i_\beta}{\mathrm{d}t} = e_\beta - v_\beta - Ri_\beta \\ C\dfrac{\mathrm{d}v_{dc}}{\mathrm{d}t} = \dfrac{3}{2}(i_\alpha d_\alpha + i_\beta d_\beta) - i_{dc} \end{cases}$$

where: i_α, i_β, v_α and v_β are the α-β axis currents and voltages on the converter side, respectively. e_α, e_β and are the AC line side voltage. The corresponding impedance on the converter side is R. L is the inductance of the smoothing reactor used in the converter side. The DC-link voltage, current, and the capacitance are v_{dc}, i_{dc}, C, respectively. d_α and d_β are the switching function. R_L is virtual load of VSC-HVDC.

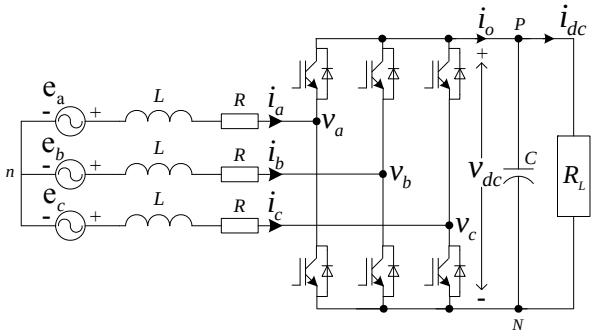

Fig.2 Power circuit of the three-phase VSC

The corresponding dynamic equation of the VSC in the rotating d-q frame can be expressed as follows [16,17]:

(2)
$$\begin{cases} L\dfrac{\mathrm{d}i_d}{\mathrm{d}t} = -Ri_d - \omega Li_q - \upsilon_{dc}d_d + e_d \\ L\dfrac{\mathrm{d}i_q}{\mathrm{d}t} = -Ri_q + \omega Li_d - \upsilon_{dc}d_q + e_q \\ C\dfrac{\mathrm{d}v_{dc}}{\mathrm{d}t} = \dfrac{3}{2}(i_d d_d + i_q d_q) - i_{dc} \end{cases}$$

From (2), the VSC-HVDC transmission system is a standard multi-input multi-output (MIMO) nonlinear system, for the existence of multiplication terms between the state variables $\{i_d,\ i_q,\ v_{dc}\}$ and the inputs control variables $\{d_\alpha, d_\beta\}$. However, this model is time invariant during a given switching state. There exists coupling of the current components between the d-axis and q-axis. In addition, the v_{dc} has to be regulated at a set point in order to maintain the DC-link voltage of the VSC-HVDC. The component e_d and e_q of direct axis and quadrature axis is regulated to zero and E_m (the peak value of AC voltage) under a balanced three phase supply, respectively. Usually, controller is based on the principle of cascade regulation. Namely, the inner fast dynamics current loop, and the outer DC voltage, slow loop.

The following section describes an input output linearization technique for the out loop. And then, a predictive current control (PCC) technique is used to obtain the inner loop controller.

DC-link voltage control with Input-Output linearization

A MIMO nonlinear system with n states and m inputs can be expressed by the state space equation as follows [10, 12]

(3) $$\dot{\mathbf{x}} = \mathbf{f}(x) + \mathbf{G}(x)\mathbf{u}$$

(4) $$\mathbf{y} = \mathbf{h}(x)$$

where: $\boldsymbol{x} \in R^n$ denotes the state, $\boldsymbol{u} \in R^m$ is the control input, $\boldsymbol{y}$ is $m \times 1$ output vector, $\boldsymbol{f}(x)$ and $\boldsymbol{h}(x)$ are nth-order smooth vector fields, and $\boldsymbol{G}(x)$ is an $n \times m$ matrix of smooth vector field columns g_i. Once the model satisfies the necessary conditions for feedback linearization, vector $\boldsymbol{h}(x) = [h_1(x),\ldots,h_m(x)]^T$, formed by the functions $\boldsymbol{G}(x)$ with a relative degree γ_i ($\gamma_1+\ldots+\gamma_m=n$), is chosen as the output vector of the system (4). An approach to obtain the IOL of the MIMO system is to differentiate the output $\boldsymbol{y}$ of the system until the inputs $\boldsymbol{u}$ explicitly appears. The smallest number of derivatives required for that γ_i is called the relative degree of that particular output. These derivatives may be expressed as follows:

(5) $$\mathbf{y}_i^{(\gamma_i)} = \mathrm{L}_f^{\gamma_i}\mathbf{h}_i + \sum_{j=1}^{m} \mathrm{L}_{g_j}\mathrm{L}_f^{\gamma_i - 1}\mathbf{h}_i\mathbf{u}_j$$

where: $\mathrm{L}_{gj}\mathrm{L}_f^{\gamma i-1}h_i \neq 0$ for at least one j in (5) if the previously mentioned condition is complied. The Lie derivative for any scalar function of h is defined as $\mathrm{L}_f\boldsymbol{h} = \nabla h \times \boldsymbol{f}$, thus, $\mathrm{L}_f^i h = \mathrm{L}_f\mathrm{L}^{i-1}{}_f\boldsymbol{h} = \nabla(\mathrm{L}^{i-1}h)\boldsymbol{f}$ is defined recursively for any positive integer i.

After performing the process to each output state variable, the following differential equation of new system is obtained:

(6)
$$\begin{bmatrix} y_1^{(\gamma_1)} \\ \vdots \\ y_m^{(\gamma_m)} \end{bmatrix} = \begin{bmatrix} \mathrm{L}_f^{\gamma_1} h_1(x) \\ \vdots \\ \mathrm{L}_f^{\gamma_m} h_m(x) \end{bmatrix} + \mathbf{E}(x) \begin{bmatrix} u_1 \\ \vdots \\ u_m \end{bmatrix}$$

or equivalently

(7) $$\mathbf{y} = \mathbf{A}(x) + \mathbf{E}(x)\mathbf{u}$$

where: the $m \times m$ decoupling matrix $\boldsymbol{E}(x)$ was defined as:

(8)
$$\mathbf{E}(x) = \begin{bmatrix} \mathrm{L}_{g_1}\mathrm{L}_f^{\gamma_1 - 1}h_1(x) & \cdots & \mathrm{L}_{g_m}\mathrm{L}_f^{\gamma_1 - 1}h_1(x) \\ \vdots & \ddots & \vdots \\ \mathrm{L}_{g_1}\mathrm{L}_f^{\gamma_m - 1}h_m(x) & \cdots & \mathrm{L}_{g_m}\mathrm{L}_f^{\gamma_m - 1}h_m(x) \end{bmatrix}$$

And then, if $\boldsymbol{E}(x)$ is nonsingular, the new transformed system with IOL can now be written as

(9) $$\mathbf{u} = \mathbf{E}^{-1}(x)\left[\boldsymbol{\upsilon} - \mathbf{A}(x)\right]$$

where: $\boldsymbol{\upsilon}$ - a dummy input vector.

Considering $\boldsymbol{\upsilon}$ as the input and $\boldsymbol{u}$ as the output of the new transformed system, it can substitute equation (9) into (7) results in a linear differential relation between the output $\boldsymbol{y}$ and the new input $\boldsymbol{\upsilon}$

(10)
$$\begin{bmatrix} y_1^{(\gamma_1)} \\ \vdots \\ y_m^{(\gamma_m)} \end{bmatrix} = \begin{bmatrix} \upsilon_1 \\ \vdots \\ \upsilon_m \end{bmatrix}$$

which is a linear differential relation between each input-output pair. Furthermore, we can see each input υ_i only affects its correspondent output $y_i^{(\gamma i)}$, so it is decoupled linear relation.

The feedback linearization is particularly useful in power electronics to solve the nonlinear problem, where a nonlinear process is transformed into a linear one by forcing the output to follow the input in a closed-loop fashion. According to the aforementioned theory of IOL, the outer loop will be derived here.

From the VSC model expressed in (2), it has only two control inputs $\boldsymbol{u} = [d_d\ d_q]^T$. Usually, d_q is used to control the

output DC-link voltage v_{dc}, and the reactive power is directly controlled by the quadrature axis current i_d which is controlled by d_d. Thus, the output states can be written as

$$\mathbf{y} = [i_q \quad v_{dc}]^T \tag{11}$$

Specialized to the two-input two-output nonlinear state equations characterizing the PWM VSC, it can obtain the corresponding vectors by substituting equation (2) into (3) with $n=3$ and $m=2$ as follows

$$\begin{bmatrix} \dot{i}_d \\ \dot{i}_q \\ \dot{v}_{dc} \end{bmatrix} = \begin{bmatrix} -\frac{R}{L} i_d - \omega i_q + \frac{e_d}{L} \\ \omega i_d - \frac{R}{L} i_q + \frac{e_q}{L} \\ \frac{3(e_d i_d + e_q i_q)}{2Cv_{dc}} - \frac{v_{dc}}{CR_L} \end{bmatrix} + \tag{12}$$

$$\begin{bmatrix} -\frac{1}{L} v_{dc} & 0 \\ 0 & -\frac{1}{L} v_{dc} \\ 0 & 0 \end{bmatrix} \begin{bmatrix} d_d \\ d_q \end{bmatrix}$$

where: $\boldsymbol{x}=[x_1, x_2, x_3]^T=[i_d, i_q, v_{dc}]^T$, $u_d= v_{dc} \times d_d$, and $u_q= v_{dc} \times d_q$. In order to make the system exact linearizable, the relative degree must be maintained. The relative degree of output v_{dc} is 2 whereas the relative degree for the i_q is 1. Thus, the total relative degree of the output state is 3 which equal to the order of the system. Furthermore, the dummy input vector can be chosen as

$$\boldsymbol{\upsilon} = \begin{bmatrix} \upsilon_1 & \upsilon_2 \end{bmatrix}^T = \begin{bmatrix} \dot{i}_q & \ddot{v}_{dc} \end{bmatrix}^T \tag{13}$$

where:

$$\ddot{v}_{dc} = \frac{3E_m \left(\dot{i}_q v_{dc} - i_q \dot{v}_{dc} \right)}{2Cv_{dc}^2} - \frac{\dot{v}_{dc}}{CR_L} \tag{14}$$

Applying the theory of IOL to the last two equations in (12), the new state equations can be obtained [18]

$$y_2^{(2)} = E(x) \left[u - \frac{3LE_m \dot{i}_q^2}{2Cv_{dc}^2} + \frac{Lv_{dc} i_q}{Cv_{dc} R_L} \right] - \frac{\dot{v}_{dc}}{CR_L} \tag{15}$$

where:

$$E(x) = \frac{3E_m}{2LCv_{dc}} \tag{16}$$

And the vector $A(X)$ in (9) is

$$A(x) = \frac{9E_m^2 i_q^2}{4C^2 v_{dc}^3} + \frac{3E_m i_q v_{dc}}{2C^2 v_{dc}^2} - \frac{\dot{v}_{dc}}{CR_L} \tag{17}$$

Thus, the out-loop of DC-link voltage can be controlled by using (9).

Inner-loop predictive current control

Assuming that the VSC works with the fixed switching frequency fs, the switching cycle is $\Delta T=1/fs$, and the time constant of VSC is much larger than the control cycle, the AC side input voltage of the VSC can be considered invariant within the adjacent switching period. With ignoring the AC side equivalent resistance, the converter side input average voltage in two-phase stationary coordinate (1) can be discretized with ΔT at samping time k as follow

$$V^{av}[k] = \varepsilon[k] + \frac{L}{\Delta T} \left\{ I^{meas}[k] - I^{meas}[k-1] \right\} \tag{18}$$

where: $[k]$ and $[k-1]$ stand for two adjacent sampling points. $I^{meas}[k]$ is the measured input AC current at time $[k]$. The control objectives of the predictive current controller is to make the actual input current at sampling point $[k+1]$ equal to the reference one

$$I_{act}[k+1] = I_{ref}[k+1] \tag{19}$$

However, the actual error between them is

$$\Delta I_{err}[k] = I_{ref}[k] - I_{meas}[k] \tag{20}$$

It can be corrected during the next control period by feed back the variables in (19) and (20) to (18) as

$$V^{av}[k] = \varepsilon[k] + \frac{L}{\Delta T} \left\{ I^{ref}[k] - I^{meas}[k] \right\} \tag{21}$$

Considering the control delay, the AC line voltage $\varepsilon[i]$ is unknown within period $[k, k+1]$. However, it can be derived by a simple linear interpolation [19]

$$\varepsilon[k] = \frac{5}{2} \varepsilon[k-1] - \frac{3}{2} \varepsilon[k-2] \tag{22}$$

Thus, combine with (21) and (22)

$$V^{av}[k] = \frac{5}{2} \varepsilon[k-1] - \frac{3}{2} \varepsilon[k-2] + \frac{L}{\Delta T} \left\{ I^{ref} - I^{meas}[k] \right\} \tag{23}$$

The measured input AC current $I^{meas}[k]$ at time $[k]$ can also be obtained by linear interpolation as follow

$$I^{meas}[k] = I^{meas}[k-1] + \frac{\Delta T}{L} \{ V^{av}[k-1] - \frac{\{3\varepsilon[k-1] - \varepsilon[k-2]\}}{2} \} \tag{24}$$

From (23) and (24), there exists

$$V^{av}[k] = 4\varepsilon[k-1] - 2\varepsilon[k-2] - V[k-1] + \frac{L}{\Delta T} \left\{ I^{ref} - I^{meas}[k-1] \right\} \tag{25}$$

Applying the same approach, the selection of interpolation coefficients for I^{ref} should consider the tradeoff between the system steady state error and transient response speed. Thus,

$$I^{ref} = I^{ref}[k+1] = \frac{9}{4} I^{ref}[k-1] - \frac{5}{4} I^{ref}[k-2] \tag{26}$$

The converter side voltage for the next switching period can be predicted from (25) and (26):

$$V^{av}[k] = 4\varepsilon[k-1] - 2\varepsilon[k-2] - V[k-1] + \frac{L}{\Delta T} \{ \frac{9}{4} I^{ref}[k-1] - \frac{5}{4} I^{ref}[k-2] - I^{meas}[k-1] \} \tag{27}$$

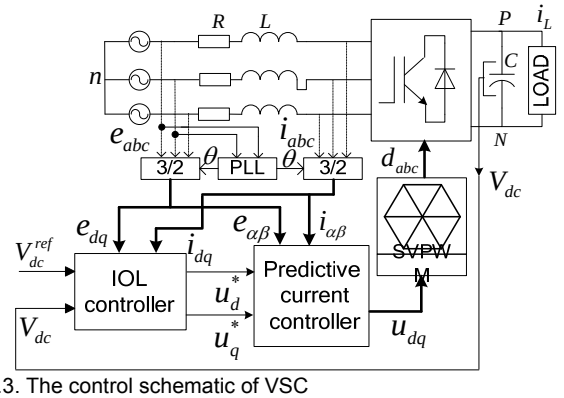

Fig.3. The control schematic of VSC

The reference voltage and current for the next period can be predicted by the measured value of two adjacent periods before. That is the principle of predictive current control. Therefore, it is easily to eliminate the static error and discretization error maximum with the help of out loop IOL control mentioned above. The control scheme is depicted in Fig.3.

Simulation results

In order to demonstrate the validity of the proposed cascaded IOL and PCC controller, a VSC-HVDC model was setup in MATLAB/Simulink environment. The parameters of the simulation model were listed in Table 1.

Table 1. Specifications of the VSC

power rating	500kVA
source Voltage E_m	10kV
DC-bus voltage V_{ref}	20kV
line inductor L	13mH
inductor resistance R	0.4Ω
dc-bus capacitor C	1500uF
AC line frequency ω	100π rad/s
switching frequency	2kHz

Fig.4 shows the steady-state waveforms of voltage and current at the VSC AC side. The converter operates under unity power factor. It is obvious that the harmonic is lower with the proposed cascaded IOL-PCC control method in Fig.4 (a) compared to the conventional PI control in Fig.4 (b).

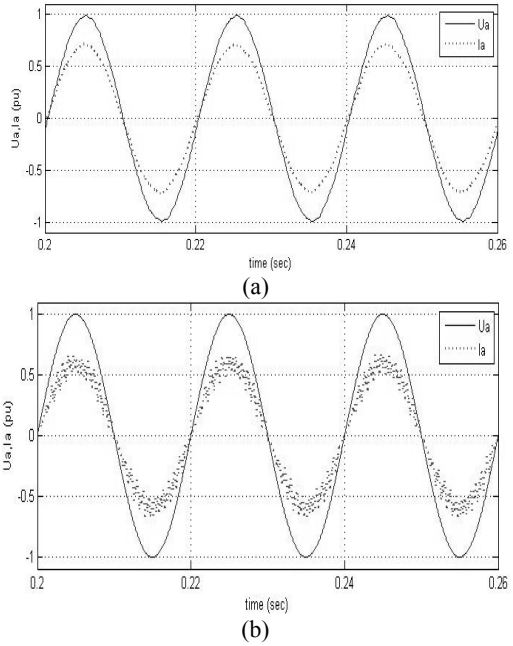

Fig.4 Voltage/current waveform of phase A. (a) the proposed IOL-PCC control, (b) conventional PI control.

In Fig.5, a smaller overshoot and fast stabilization can be achieved with IOL out loop control, compared to the conventional PI control. Moreover, the controller with the proposed methods in this paper can follow the change of reference quickly. It can be seen the good feature of the proposed IOL-PCC method.

Fig.6 shows the situation of power flow reverse happening at 0.4s with the active power changes from 0.5pu to -0.5pu, where VSC working conditions interchange from invert to rectify. The DC-link voltage drops 10% as shown in Fig.6 (a). But, it can recover to the setting point within 0.04s. The current of d-axis and q-axis is decoupled as shown in Fig.6 (b). And with the fast current tracking ability in the inner current loop, the d-axis current are regulated to the new setting point quickly. The voltage and current of VSC side phase A is shown in Fig.6 (c). The DC-link current inverse under this working condition is shown in Fig.6 (d).

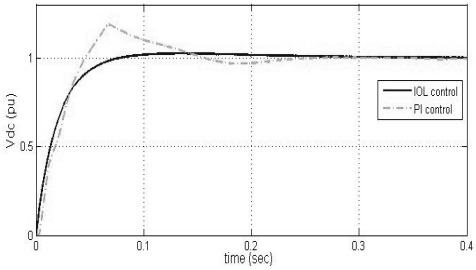

Fig. 5 DC-link voltage responses under different control scheme.

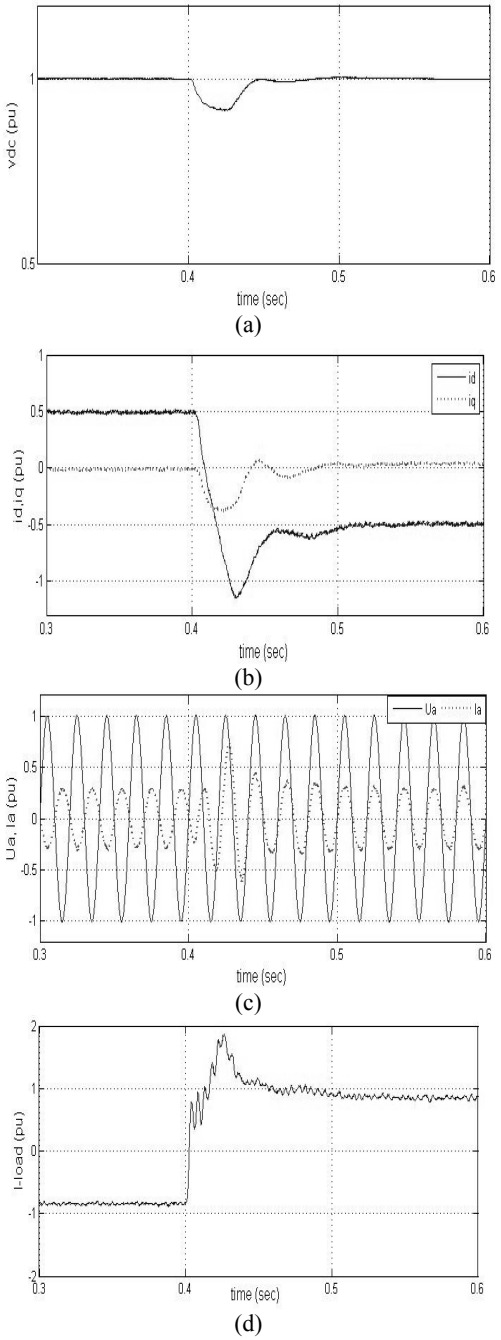

Fig.6 Responses of power flow reverse. (a) DC-link voltage, (b) Decoupled d-q axis currents, (c) Ac side voltage/current, (d) DC-link current.

Conclusion

In this paper, a nonlinear control method based on IOL and PCC for VSC-HVDC transmission system has been presented. The nonlinearity of the system and the coupling effect the d-q current control were eliminated by the proposed cascaded control scheme. The PCC technology can eliminate the delay caused by sampling and calculation, improve the current response speed, and reduce the input current harmonic content.

Simulation results have verified the validity and effective of the proposed control scheme. These results show the satisfactory performance of the proposed IOL-PCC controller in comparison to the traditional PI controller. Also, the results in this paper can further be an effective scheme in the hardware design of digital control system based on floating point DSP devices.

Acknowledgment

This Project was granted financial support from Key Project of National Science Foundation of China (60934005), Shanghai Education Development Foundation (09LM37,10LM26), and Shanghai Scientific Development Foundation (09195802900).

REFERENCES

[1] Nogal, L., Stability enhancing control of HVDC connection, *Przeglad Elektrotechniczny*, 88 (2012), No. 3A, 121-124

[2] Dong-Choon L., G-Myoung L., and K.-D. L., DC-Bus Voltage Control of Three-Phase AC DC PWM Converters Using Feedback Linearization, *IEEE Transactions On Industry Applications*, 36 (2000), No. 3, 826-833

[3] Du, C.Q., Agneholm E., and Olsson G., VSC-HVDC System for Industrial Plants With Onsite Generators, *IEEE Transactions on Power Delivery*, 24 (2009), No. 3, 1359-1366

[4] Abbas A.M., and Lehn P.W., PWM Based VSC-HVDC Systems - a Review, *IEEE Power & Energy Society General Meeting*, 1-8 (2009), 4478-4486

[5] Weixing, L., and O. Boon-Teck, DC overvoltage control during loss of converter in multiterminal voltage-source converter-based HVDC (M-VSC-HVDC), *IEEE Transactions on Power Delivery*, 18 (2003), No. 3, 915-920

[6] Zhou K.L., and Wang D.W., Relationship between space-vector modulation and three-phase carrier-based PWM: A comprehensive analysis, *IEEE Transactions On Industrial Electronics*, 49 (2002), No. 1, 186-196

[7] Wang F., Sine-Triangle versus Space-Vector Modulation for Three-Level PWM Voltage-Source Inverters, *IEEE Transactions On Industry Applications*, 38 (2002), No. 2, 500-506

[8] Guo-Qiang W., Zhi-Xin W., Control of HVDC-light transmission for offshore wind farms based on input-output feedback linearization and PSO, *WSEAS Transactions on Systems*, 9 (2010), No. 11, 1109-1119

[9] Isidori A., Nonlinear Control Systems, *Germany: Springer-Verlag*, 1989, Berlin

[10] Slotine J.E., and Li W., Applied Nonlinear Control, *Englewood Cliffs*, *NJ: Prentice-Hall*, 1991.

[11] Daizhan C., Applied Nonlinear Control, *China Machine Press, China*, 2009.

[12] Moharana A., and Dash P.K., Input-Output Linearization and Robust Sliding-Mode Controller for the VSC-HVDC Transmission Link, *IEEE Transactions on Power Delivery*, 25 (2010), No. 3, 1952-1961

[13] Tzann-Shin L., Input-output linearization and zero-dynamics control of three-phase AC/DC voltage-source converters, *IEEE Transactions on Power Electronics*, 18 (2003), No. 1, 11-22

[14] Jeong S., and Song S., Improvement of Predictive Current Control Performance Using Online Parameter Estimation in Phase Controlled Rectifier, *IEEE Transactions On Power Electronics*, 22 (2007), No. 5, 1820-1825

[15] Blasko V., Kaura V., A New Mathematical Model and Control of a Three-Phase AC-DC Voltage Source Converter, IEEE Transactions on Power Electronics, 12 (1997), No. 1, 116-123

[16] Burgos R.P., Wiechmann E.P., and Holtz J., Complex state-space modeling and nonlinear control of active front-end converters, *IEEE Transactions on Industrial Electronics*, 52 (2005), No. 2, 363-377

[17] Yongsug S., Tijeras V., and Lipo T.A., A Nonlinear Control of the Instantaneous Power in dq Synchronous Frame for PWM AC/DC Converter under Generalized Unbalanced Operating Conditions, *IEEE Industry Applications Society Conference*, 2 (2002), 1189-11496

[18] D.C. Lee, Advanced nonlinear control of three-phase PWM rectifiers, *IEE Proceedings - Electric Power Applications*, 147 (2000), No. 5, 361-366

[19] Holmes D., Martin D., Implementation of a direct digital predictive current controller for single and three phase voltage source inverters, *IEEE IAS-96 Annual Meeting,* San Diego,1996, 906-913

[20] Kebbati I., Hammou Y., Mansouri A., et al., Sliding mode control with a robust observer of induction motor, *Przeglad Elektrotechniczny*, 88 (2012), No. 1B, 193-197

Authors:

Dr. Shuang LI: Shanghai Jiaotong University. M.B.0903191, 800#, Dongchuan Road, Shanghai, China. E-mail: cooleels@126.com

Prof. Zhixin WANG: Shanghai Jiaotong University, Shanghai, China.

Dr. Guoqiang WANG: Shanghai Jiaotong University, Shanghai, China. E-mail: cock_wgq@126.com.